Boundary-Layer Meteorol (2017) 165:145–160
DOI 10.1007/s10546-017-0260-3

RESEARCH ARTICLE

# Estimation of Surface-Layer Scaling Parameters in the Unstable Boundary Layer: Implications for Orographic Flow Speed-Up

**José Luís Argaín**[1] · **Miguel A. C. Teixeira**[2] · **Pedro M. A. Miranda**[3]

Received: 12 August 2016 / Accepted: 2 May 2017 / Published online: 5 June 2017


**Abstract** A method is proposed for estimating the surface-layer depth ($z_s$) and the friction velocity ($u_*$) as a function of stability (here quantified by the Obukhov length, $L$) over the complete range of unstable flow regimes. This method extends that developed previously for stable conditions by Argaín et al. (Boundary-Layer Meteorol 130:15–28, 2009), but uses a qualitatively different approach. The method is specifically used to calculate the fractional speed-up ($\Delta S$) in flow over a ridge, although it is suitable for more general boundary-layer applications. The behaviour of $z_s$ ($L$) and $u_*$ ($L$) as a function of $L$ is indirectly assessed via calculation of $\Delta S$ ($L$) using the linear model of Hunt et al. (Q J R Meteorol Soc 29:16–26, 1988) and its comparison with the field measurements reported in Coppin et al. (Boundary-Layer Meteorol 69:173–199, 1994) and with numerical simulations carried out using a non-linear numerical model, FLEX. The behaviour of $\Delta S$ estimated from the linear model is clearly improved when $u_*$ is calculated using the method proposed here, confirming the importance of accounting for the dependences of $z_s$ ($L$) and $u_*$ ($L$) on $L$ to better represent processes in the unstable boundary layer.

**Keywords** Convective boundary layer · Flow speed-up · Friction velocity · Surface-layer height · Unstable stratification

✉ José Luís Argaín
jargain@ualg.pt

Miguel A. C. Teixeira
m.a.teixeira@reading.ac.uk

Pedro M. A. Miranda
pmmiranda@fc.ul.pt

[1] Departamento de Física, FCT, Universidade do Algarve, 8005-139 Faro, Portugal

[2] Department of Meteorology, University of Reading, Earley Gate, PO Box 243, Reading RG6 6BB, UK

[3] Instituto Dom Luiz, Faculdade de Ciências, Universidade de Lisboa, 1749-016 Lisbon, Portugal

## 1 Introduction

Fractional speed-up ($\Delta S$) of flow over hills or mountains is defined as the ratio of the speed perturbation at a given height to the upstream, unperturbed flow speed at the same height. This quantity is highly relevant both from meteorological and wind engineering perspectives, since it characterizes the modulation of the wind speed by orography. Hunt et al. (1988) (hereafter HLR) developed one of the first theoretical linear atmospheric boundary-layer (ABL) models of flow over hills, which is one of the simplest and computationally cheapest tools available for estimating $\Delta S$. However, stratification affects $\Delta S$ and must be carefully accounted for in the evaluation of the scaling parameters that characterize the ABL. Among these, a key parameter is the friction velocity ($u_*$), and another is the surface-layer depth ($z_s$), usually estimated as 5–10% of the ABL depth.

Weng (1997) (hereafter W97), after implementing a continuous wind profile in the HLR model, found that his predictions of $\Delta S$ disagreed significantly with the observations of Coppin et al. (1994) (hereafter C94). Argaín et al. (2009) (hereafter A09) showed that these discrepancies were due to the fact that the calculations in W97 were carried out assuming that $u_*$ is constant, regardless of the different observed stability regimes. They proposed a method for estimating $u_*$ in stably-stratified flows, which has led to an improved prediction of $\Delta S$ over two-dimensional (2D) hills. C94 also compared their observations with predictions from the HLR model, and found considerable disagreement, both in stable and unstable conditions. Here, we show that, as in stably-stratified flows, a decisive reason for such disagreements in unstable flow is the assumption of constant $u_*$.

In the present study, a new method is developed for estimating $z_s$ and $u_*$ as a function of stability (here quantified by the Obukhov length, $L$) over the complete unstable stratification range, i.e. from the free-convection to the neutral stability limits. Procedures are developed for estimating $z_s$ in a neutral ABL, and for estimating this and several other scaling parameters, such as $u_*$, $L$ and Deardorff's convective velocity scale, $w_*$, in the free-convection regime, which are preliminary steps for defining $z_s(L)$ and $u_*(L)$ for all stabilities. Given that the physical processes taking place in the convective boundary layer (CBL) and in an unstable surface layer are substantially different from those in a stable ABL, the method used to represent them also differs substantially, requiring the use of additional theory.

The main motivation for developing this new method for estimating $z_s(L)$ and $u_*(L)$ is the calculation of $\Delta S(L)$ for unstable flow over hills, although it must be noted that the method can also be used for more general boundary-layer applications. The calculation of $\Delta S(L)$ requires knowledge of $u_*(L)$, which, in the method proposed here, also requires estimating $z_s(L)$. The behaviour of $z_s(L)$ and $u_*(L)$ is thus indirectly assessed through the calculation of $\Delta S(L)$ using the HLR model. These predictions are compared with field measurements reported in C94, and numerical simulations carried out using a 2D microscale–mesoscale non-hydrostatic model, FLEX. These comparisons allow us to show how $z_s(L)$ and $u_*(L)$ are sometimes not estimated in a physically consistent way, a limitation that the present method aims to overcome.

Section 2 presents the method that accounts for unstable stratification in the ABL and its calibration, while Sect. 3 describes the main results, namely comparisons between theory, numerical simulations and measurements, using the new unstable ABL formulation. Finally, Sect. 4 summarizes the main conclusions.

## 2 Methodology

### 2.1 Unstable ABL Model

Several studies show that the ABL, under moderate to strong unstable stratification (usually known as the CBL), can be represented as a simplified three-layer bulk model (e.g. Garratt 1992). This comprises a thin statically unstable surface layer of depth $z_s$, a well-mixed layer, of height $z_i$ and depth $\Delta z_i = z_i - z_s$, and a transition layer of thickness $\Delta z_{ci}$, coinciding with a temperature inversion capping the mixed layer, which inhibits vertical mixing. In the mixed layer, quantities such as the mean potential temperature ($\theta$) and wind velocity ($U$, $V$) are well-mixed, and therefore constant with height, i.e. $\theta\,(z) = constant$, $U\,(z) = constant$ and $V\,(z) = 0$. For our purposes, the strict fulfilment of these profile shapes in the mixed layer is not critical, since we are essentially interested in the surface layer, for which typically $z_s \approx 0.05 z_i$ to $0.1 z_i$ (Stull 1988). In the surface layer we assume that the turbulent shear stresses have a more important effect on the mean flow than does the Coriolis force. Hence, the Coriolis parameter ($f$) is set to zero, except where otherwise explicitly stated. Since the surface layer has characteristics that make it markedly different from the mixed layer, $z_s$ can be defined as an important length scale of the ABL, essential for describing the impact of the orography on the wind profile. This follows McNaughton (2004), who established $z_s$ as a new basis parameter for similarity models of the surface layer. In the method proposed here, $z_s$ is essential for estimating the key velocity scale, $u_*$, and hence for calculating $\Delta S\,(L)$.

### 2.2 Surface-Layer Model

According to Monin–Obukhov similarity theory (MOST), in the surface layer the non-dimensional vertical gradients of $U\,(z)$ and $\theta\,(z)$ are universal functions of the parameter $z/L$, taking the forms

$$\Phi_m\left(\frac{z}{L}\right) = \frac{\kappa z}{u_*}\frac{\partial U}{\partial z}, \tag{1}$$

and

$$\Phi_h\left(\frac{z}{L}\right) = \frac{\kappa z}{Pr_t \theta_*}\frac{\partial \theta}{\partial z}, \tag{2}$$

where $z$ is the height above the effective ground level, $\kappa$ is the von Kármán constant, $Pr_t$ is the turbulent Prandtl number and $\theta_*$ represents the surface-layer scaling temperature. Here, $u_*$ and $\theta_*$ are defined using the vertical eddy kinematic fluxes of momentum and heat at the surface, i.e. $u_*^2 = -\left(\overline{w'u'}\right)_0$ and $\theta_* = -\left(\overline{w'\theta'}\right)_0 / u_*$. The length scale $L$ is given by

$$L = -\frac{\theta_0 u_*^3/\kappa}{g\left(\overline{w'\theta'}\right)_0} = \frac{\theta_0 u_*^2}{g\kappa\theta_*}, \tag{3}$$

where $\theta_0$ is the potential temperature at the surface and $g$ is the acceleration due to gravity. Wilson (2001) (hereafter W01), after analyzing several forms of the functions $\Phi_m$ and $\Phi_h$, proposed the following general form for the unstable regime ($z/L < 0$),

$$\Phi = \left(1 + \gamma\left|\frac{z}{L}\right|^{\alpha_1}\right)^{-\alpha_2}, \tag{4}$$

which is valid for both $\Phi_m$ and $\Phi_h$. He noted that in order to obtain the correct physical behaviour for the gradients $\partial U/\partial z$ and $\partial\theta/\partial z$ in the free-convection limit ($z/L \to -\infty$), it

is required that $\alpha_1\alpha_2 = 1/3$. For this combination of values (4) behaves in this limit similarly to 'classical' free-convection expressions, with $\partial U/\partial z$ and $\partial\theta/\partial z$ varying as $z^{-4/3}$. He further noted that, for this choice of parameters, (1)–(2) may be integrated straightforwardly. Following W01 we use $\kappa = 0.4$, $Pr_t = 0.95$, $\gamma_h = 7.86$, $\alpha_{1m} = \alpha_{1h} = 2/3$, $\alpha_{2m} = \alpha_{2h} = 1/2$ and $\gamma_m = 3.59$.

Subscripted indices $s$, $n$ and $fc$ hereafter denote values of flow parameters in the surface layer, in the neutral regime ($|L| \to \infty$), and in the free-convection regime ($|L| \to 0$), respectively. The method developed here requires that $z_{sfc}$, $u_{*fc}$, $L_{fc}$, $z_{sn}$, $u_{*n}$ and $z_0$, be known in order to calculate $u_*(L)$ and $z_s(L)$. The primary input parameters are $u_{*n}$, $z_{ifc}$ and the aerodynamic roughness length, $z_0$, which must be provided initially.

### 2.3 Estimating Parameters in the Free-Convection and Neutral Regimes

MOST shows good agreement with observations in regimes with sufficiently high wind speeds (high values of $u_*$) or under relatively low surface heat flux, $\left(\overline{w'\theta'}\right)_0$, where $|L| > 10^2$ m. This theory is based on the assumption that, in the surface layer, $z$ and $L$ are the only relevant length scales. While this assumption is valid for relatively small values of $|z/L|$ (say $|z/L| < 0.1$), for larger values, in particular in the free-convection regime, MOST becomes incomplete. In the perfectly windless regime, purely dominated by thermal effects, both the mean wind speed and $u_*$ approach zero, and MOST produces singularities and underestimates the surface fluxes. However, perfectly windless conditions occur very rarely, and the theory can still be applied, if conjugated with CBL theory, for low but non-zero wind speeds, as will be shown below.

For the highly convective ABL, Deardorff (1970) suggested the following convective velocity scale

$$w_* = \left[\frac{g}{\theta_0}\left(\overline{w'\theta'}\right)_0 z_{ifc}\right]^{1/3}. \tag{5}$$

The combination of MOST and Deardorff similarity theory, adopted here, provides a model that is consistent throughout the whole CBL (Kaimal et al. 1976) (hereafter K76), and for stabilities ranging from the neutral regime to the free-convection regime. This latter regime does not strictly correspond to $L = 0$, but rather to a minimum, suitably small, value of $L = L_{fc}$ to be determined. In the free-convection regime we need to estimate $z_{sfc}$, $u_{*fc}$, and $L_{fc}$, and given that $u_{*fc}$ is defined in relation to $w_*$ (as shown below), this latter quantity, defined by (5), must also be related to the known input parameters. This requires a total of four equations (see below).

Many observations have confirmed that the transition from the shear-driven turbulent regime of the surface layer to the buoyancy-driven regime of the mixed layer usually occurs at a height of order $|L|$. Hence, in a highly convective ABL (Garratt 1992),

$$z_{sfc} = c_{fc}\left|L_{fc}\right|, \tag{6}$$

where $c_{fc} = 2$, and Eq. 6 is adopted hereafter in the free-convection regime.

Based on observations, Schumann (1988) (hereafter S88) assumed that $z_s/z_i = 0.1$. As will be seen later, this assumption is too restrictive over the whole stability interval, since $z_i$ is expected to increase and $z_s$ to decrease as the stratification becomes more unstable. A more general definition of $z_s$ is thus required, to be developed in Sect. 2.4.

Businger (1973) proposed the idea that $u_*$ does not vanish at low wind speeds, introducing the concept of a 'minimum friction velocity', valid in the free-convection regime ($u_{*min} = u_{*fc}$). Combining (3) and (5) in this regime, we obtain

$$\frac{\kappa \left| L_{fc} \right|}{z_{ifc}} = \left( \frac{u_{*fc}}{w_*} \right)^3, \tag{7}$$

and using (6), it can be easily shown from (7) that $z_{sfc}/z_{ifc}$ decreases as $u_{*fc}/w_*$ decreases, which is physically plausible.

Various authors, such as S88 and Sykes et al. (1993) (hereafter S93), have advocated the view that $u_{*fc}/w_*$ is a function of $z_{sfc}/z_0$ or $z_{ifc}/z_0$ as well. Following the less general relations derived by S88 and S93, valid only for limited intervals of $z_0$, Zilitinkevich et al. (2006) (hereafter Z06) suggested a more complete formulation for the relationship between $u_{*fc}/w_*$ and $z_{ifc}/z_0$, which takes into account the combined effects of buoyancy and shear forces,

$$\frac{u_{*fc}}{w_*} = c_1 \left[ \ln \frac{z_{ifc}/z_0}{\left( \ln z_{ifc}/z_0 - c_0 \right)^3} + c_2 \right]^{-1} \quad \text{for } \geq \sigma, \tag{8}$$

$$\frac{u_{*fc}}{w_*} = c_3 \left[ \frac{z_0}{z_{ifc}} + c_4 \left( \frac{z_0}{z_{ifc}} \right)^{8/7} \right]^{1/6} \quad \text{for } < \sigma, \tag{9}$$

where $\sigma = 3.45 \times 10^5$, $u_{*fc}/w_*(\sigma) = 0.065$, $c_0 = 6.00$, $c_1 = 0.29$, $c_2 = -2.56$, $c_3 = 0.54$ and $c_4 = 0.3$. Equations 8 and 9 agree very well with both LES and field data in the free-convection regime (Z06), and incorporate the best characteristics of the S88 and S93 models.

The height $z_i$ characterizes the PBL in a fairly integrated manner, being closely related to fundamental quantities such as $\left( \overline{w'\theta'} \right)_0$. For this reason, as a first approach, we suggest estimating surface-layer scaling parameters in the free-convection regime based on a known value of $z_{ifc}$. This allows obtaining $u_{*fc}/w_*$ directly from (8)–(9), since $z_0$ is also assumed to be known.

Our final constraint is based on Venkatram (1978) who, by using a simple mixed-layer model for the CBL, derived the following relationship between $w_*$ and $z_{ifc}$,

$$w_* = c_5 z_{ifc}, \tag{10}$$

where $c_5 = 1.12 \times 10^{-3}$ s$^{-1}$. Equation 10 compares extremely well with observations (see "Appendix 2"), and using the available value of $z_{ifc}$, (10) allows us to determine $w_*$ directly.

Equations 6–10 may thus be used to obtain the surface-layer parameters in the free-convection regime, as follows. Given $z_{ifc}$ and $z_0$, (8) or (9) is used to obtain $u_{*fc}/w_*$ and (10) is used to obtain $w_*$, which yields $u_{*fc}$. Given $z_{ifc}$, $w_*$ and $u_{*fc}$, determined in the preceding step, (7) is used to obtain $L_{fc}$. Finally, $L_{fc}$ is inserted into (6) to obtain $z_{sfc}$, yielding $u_{*fc}$, $L_{fc}$, and $z_{sfc}$, as required. Several different procedures analogous to that just described would be possible, depending on the input parameters known initially.

According to MOST, in the neutral regime

$$U_n(z) = \frac{u_{*n}}{\kappa} \ln \left( \frac{z}{z_0} \right). \tag{11}$$

Since, from (6), $z_s$ is expected to depend on $L$, in the neutral regime at least (where no stability effects exist), it seems reasonable to assume $z_s$ to be a fixed fraction of $z_i$ (Stull 1988),

$$z_{sn} = c_{SL} z_{in}, \tag{12}$$

where that fraction is conventionally defined as 5–10% of $z_i$ (Stull 1988). In our model, we assume $c_{SL} = 0.05$ (following Stull 2011). Here, and unlike the practise of previous authors, (12) is adopted only for the strictly neutral regime. As will be seen later (Sect. 3.2), (12) holds approximately for a weakly unstable ABL, but not for a strongly unstable ABL. In order to obtain $z_{sn}$ from (12), it is still necessary to estimate $z_{in}$. This can be done using the expression of Rossby and Montgomery (1935),

$$z_{in} = \frac{c_{zin} u_{*n}}{|f|}, \tag{13}$$

where $c_{zin} = 0.2$ (Garratt 1992).

### 2.4 Estimating $z_s$ and $u_*$ for Arbitrary $L < 0$

The preceding section described the methodologies for estimating all the parameters required for defining $u_*$ and $z_s$ in the free-convection and neutral regimes. Next we explain the approach used to estimate these two parameters for arbitrary $L<0$.

Since $|L|$ is the height at which the buoyant production of turbulence kinetic energy (TKE, or $E$) begins to dominate over shear production, the greater is $(\overline{w'\theta'})_0$ (i.e. the smaller is $|L|$), the bigger is $\Delta z_i$ and the smaller $z_s$ becomes, because convectively-driven turbulence increasingly dominates over shear-driven turbulence. So, there is a clear relationship between $z_s$ and $|L|$ [expressed by (6) in the strongly unstable regime]. However, for intermediate unstable regimes the dependence $z_s(L)$ is not known.

Based on the ABL model described in Sect. 2.1, we define $z_s$ as the height at which the vertical derivative of $\theta(z)$ reaches a small prescribed fraction of its surface value. Using this property, in the present model $z_s(L)$ is determined by (see details in "Appendix 1") evaluating the root of,

$$\frac{z_s}{z_{0\theta}} = \frac{1}{\alpha_{\Psi 2}} \left( \frac{z_{0\theta}}{z_s} \right)^{-\alpha_{\Psi 1}} \left[ \frac{1 + \gamma_h \left( z_s / |L| \right)^{\alpha_1}}{1 + \gamma_h \left( z_{0\theta} / |L| \right)^{\alpha_1}} \right]^{-\alpha_2}, \tag{14}$$

for any value of $L$, assuming that $z_{0\theta}$, $\alpha_1$, $\alpha_2$, $\gamma_h$, $\alpha_{\Psi 1}$ and $\alpha_{\Psi 2}$ are provided. As (14) includes the influence on $z_s(L)$ of parameters in both extremes of the stability interval (see "Appendix 1"), it is expected to provide a good approximation over the whole stability range. As the roughness length for heat, $z_{0\theta}$, is not provided by C94, we use here $z_0$ instead. Calculations not presented here show that the $z_s(L)$ dependences obtained using $z_{o\theta}/z_s$ or $z_o/z_s$ are quite similar (the relation between $z_{o\theta}$ and $z_o$ assumed for this comparison follows Zilitinkevich 1995). Although $z_{o\theta}$ and $z_o$ differ, the proposed method for estimating $z_s$ is not very sensitive to the exact value of $z_o$ so long as this is small; $u_*(L)$, on the other hand, is calculated from

$$u_*(z_s, L) = \kappa z_s \left[ 1 + \gamma_m \left( \frac{z_s}{|L|} \right)^{\alpha_1} \right]^{\alpha_2} \left( \frac{\partial U}{\partial z} \right)_{Z_s}, \tag{15}$$

where, in accordance with the slab model adopted initially (see Sect. 2.1), it is expected that $\partial U/\partial z$ becomes small as $z \to z_s$. Here we assume that in (15) the shear $(\partial U/\partial z)_{z_s}$ is constant, and, for convenience, equal to its neutral value. For $|L| \to \infty$ and at $z = z_s$, (1)

reduces to $(\partial U/\partial z)_{z_{sn}} = u_{*n}/(\kappa z_{sn})$, in accordance with (11), where $z_{sn}$ may be obtained from (12). The validity of the assumption $(\partial U/\partial z)_{z_s} = constant$ is tested in "Appendix 2".

All quantities on the right-hand side of (15) are now known, and hence $u_*(z_s, L)$ may be determined in general. Finally, the $U(z)$ profile for the general unstably–stratified case, which will be used in the HLR model for calculating $\Delta S(L)$,

$$U(z) = \frac{u_*}{\kappa}\left\{\ln\left(\frac{z}{z_0}\right) - 3\ln\left[\frac{1+\sqrt{1+\gamma_m\,(z/|L|)^{2/3}}}{1+\sqrt{1+\gamma_m\,(z_0/|L|)^{2/3}}}\right]\right\}, \tag{16}$$

is obtained by integration of (1), using the velocity gradient expressed by (4) (see W01).

In the above treatment, it is assumed that the synoptic situation does not vary too rapidly compared with the time scales of flow over the ridge. Hence, according to MOST, the effect of $L$ in the surface layer is dominant. As this quasi-steadiness is supported by the C94 campaign, the C94 observations can safely be used for testing the proposed method. For more unsteady flows, it is likely necessary to use a time-dependent model for the whole ABL, such as that described by Weng and Taylor (2003), for providing upstream profiles $U(z)$ and $\theta(z)$ at different values of $L$. However, this approach would require more input parameters not available in the C94 observations, and their estimation would further increase the empiricism of the proposed method.

Summarizing, in this section, assuming that $z_0$, $z_{sfc}$, $L_{fc}$, $z_{sn}$ and $u_{*n}$ are known, we propose (14) and (15) for determining $z_s(L)$ and $u_*(L)$, respectively; $u_*(L)$ is then used in the HLR model to calculate $\Delta S(L)$ for flow over orography.

## 3 Results and Discussion

The method presented above is assessed using the observations of C94. These measurements were conducted during the spring 1984 and summer 1985, over Cooper's Ridge, located to the north–west of Goulburn, in New South Wales, Australia. This is a somewhat isolated north–south oriented, quasi-two-dimensional ridge of uniform low $z_0$, located along a valley that forces flow over the hill predominantly from the west side. The windward slope of the ridge (west side) can be well fitted using a simple bell-shaped profile $h(x) = h_0/\left\{1+(x/a)^2\right\}$ (with $h_0 = 115$ m and $a = 400$ m), while the lee side of the ridge falls away to about $0.5h_0$ before rising to another broader ridge.

### 3.1 Estimation of Parameter Values From the Data

As mentioned in Sect. 2, for determining $z_s(L)$ and $u_*(L)$, the method developed here requires that $z_0$, $z_{sfc}$, $u_{*fc}$, $L_{fc}$, $z_{sn}$ and $u_{*n}$ be known. From the data collected by C94, we have $u_{*n} = 0.35$ m s$^{-1}$, $z_0 = 0.05$ m and $f \approx 9\times10^{-5}$ s$^{-1}$. Using (13) we thus obtain $z_{in} = 778$ m. Using this value in (12) yields $z_{sn} = 39$ m.

The methodology described in Sect. 2.3 for estimating the flow parameters in the free-convection regime ($z_{sfc}$, $u_{*fc}$, $L_{fc}$ and $w_*$) is now applied. As $z_{ifc}$ is not supplied by C94, we use a typical value corresponding to the season and latitude of the region where the observations were taken. Figures containing the necessary information from the ERA-40 Reanalysis provided by Von Engeln and Teixeira (2013) suggest $z_{ifc} = 1550$ m. Next, since $z_{ifc}/z_0 = 3\times10^4 < \sigma = 3.45\times10^5$, we must use (9) to calculate $u_{*fc}/w_* = 0.098$. Substituting $u_{*fc}/w_*$ and $z_{ifc}$ into (7), we obtain $L_{fc} = -3.6$ m, and from (6) we obtain

**Table 1** Parameters of the ABL in the free-convection regime

| Source | $u_{*fc}$ (m s$^{-1}$) | $\|L_{fc}\|$ (m) | $z_{sfc}$ (m) | $z_{ifc}$ (m) | $z_{sfc}/z_{ifc}$ | $w_*$ (m s$^{-1}$) | $u_{*fc}/w_*$ |
|---|---|---|---|---|---|---|---|
| Present method | 0.17 | 3.6 | 7.2 | 1550 | 0.005 | 1.70 | 0.098 |
| Run 6A1 | 0.24 | 5.7 | 10.4 | 2095 | 0.005 | 2.43 | 0.099 |
| Run 6A2 | 0.23 | 6.4 | 12.8 | 2035 | 0.006 | 2.21 | 0.104 |

*Line* 1: parameters used in the present method. *Lines* 2–3: similar parameters from runs 6A1 and 6A2 of the experiment described in Kaimal et al. (1976). The value of $z_{sfc}$ for these runs was obtained from (6)

$z_{sfc} = 7.2$ m. Next, substitution of $z_{ifc}$ in (10) gives $w_* = 1.74$ m s$^{-1}$, which in turn can be used for calculating $u_{*fc}$ from $u_{*fc}/w_* = 0.098$, yielding $u_{*fc} = 0.17$ m s$^{-1}$. Table 1 presents known and estimated parameters of the ABL in the free-convection regime, obtained by the present method and, for comparison, observations from runs 6A1 and 6A2 of the field experiment reported by K76, corresponding to a highly convective ABL. As can be seen, the method proposed here seems to predict realistic results.

It is interesting that, in contrast to what happens in the neutral regime, the ratio $z_{sfc}/z_{ifc} = 0.005$ estimated above is significantly lower than the value assumed in (12). This value is of the same order of magnitude as values derived from the measurements of K76, taken in strongly convective conditions (see Table 1). As pointed out before, the smaller is $|L|$, the more intense the turbulent mixing by large convective eddies in the mixed layer becomes, thereby reducing $z_s$. This corroborates, using real data, that the neutral approximation for $z_{sn}/z_{in}$ cannot be considered realistic over the whole range of variation of $L$, particularly near the free-convection regime.

### 3.2 Behaviour of $z_s$ as a Function of $L$

For a better understanding of the surface-layer structure, it is useful to define a transition height, $z_{tr}$, at which the convective contribution to $U(z)$ is as important as that of the neutral logarithmic law. Following Kader and Yaglom (1990), from the W01 formulation (4) we can define

$$z_{tr} = |L|\,\gamma_m^{-1/\alpha_1}. \tag{17}$$

It is expected that, in moderately to strongly unstable flow regimes $z_{tr} < z_s$, i.e. at the top of the surface layer $U(z)$ is no longer logarithmic (in fact, this generally happens in non-neutral conditions).

Figure 1 presents the variation of $z_s$ and $z_{tr}$, with $|L|$, normalized by $z_{sn}$, where the solid line represents $z_s(L)$, computed using (14). In (14), the coefficients $\alpha_{\Psi 1}$ and $\alpha_{\Psi 2}$, given by (23), take the values 0.415 and 0.018, respectively. $z_{tr}(L)$ (dashed line) is computed using (17).

The dotted vertical lines correspond to $|L_{fc}| = 3.6$ m (left) as determined previously (see Table 1), and the value of $|L_{tr}| = 120$ m (right) for which $z_s(L) = z_{tr}(L)$, i.e. for which the logarithmic and convective contributions to $U(z)$ are equally important. For $|L| > 400$ m, the logarithmic portion of $U(z)$ is overwhelmingly dominant compared to the convective one, and therefore it can be considered that the ABL is in near-neutral conditions. For $L = L_{fc}$ or lower, the opposite is true, as the flow is close to free-convection conditions; $z_s(L)$ physically behaves as expected, tending asymptotically to constant values at each extreme of the stability interval (4.5 m as $|L| \to 0$, and $z_{sn}$ for $|L| \to \infty$). Figure 1 illustrates the way

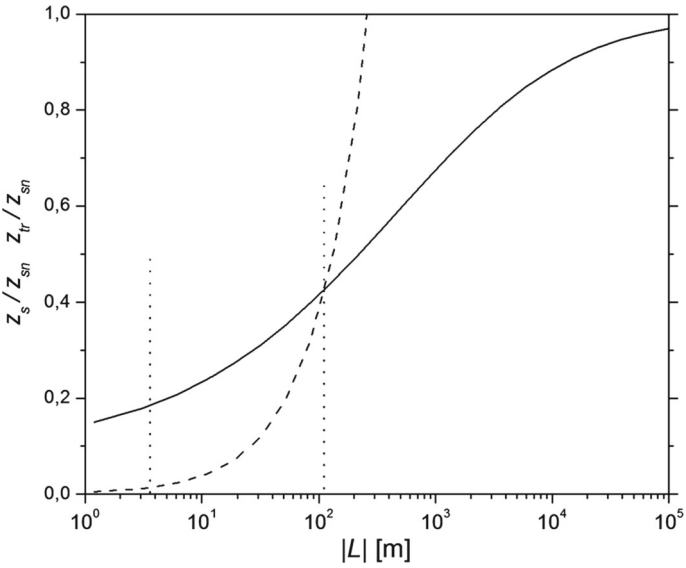


**Fig. 1** Surface-layer height, $z_s$, and transition height, $z_{tr}$, as a function of $|L|$, normalized by the surface-layer height for a neutral ABL, $z_{sn}$. *Solid line*: $z_s(L)$ obtained from (14), dashed line: $z_{tr}(L)$ obtained from (17). *Vertical dotted lines*: $|L_{fc}| = 3.6$ m (*left*), and $|L_{tr}| = 120$ m (*right*). $z_s(L)$ asymptotically approaches the constant values $z_{sn}$ as $|L| \to \infty$ and $z_s(L) = 4.5$ m as $|L| \to 0$. $z_s\left(L_{fc}\right) = z_{sfc} = 7.2$ m (see Table 1)

in which the surface-layer depth decreases with increasing unstable stratification, because of the progressively higher buoyant production of TKE in the mixed layer as $|L|$ decreases.

### 3.3 Behaviour of $u_*$ as a Function of $L$

Figure 2 presents $u_*$ as a function of $|L|$, normalized by $u_{*n}$. The solid line corresponds to $u_*(L)$ computed from (15), and the dash-dotted line extends the constant neutral value, $u_{*n} = 0.35$ m s$^{-1}$, over the whole stability interval, for comparison. Figure 2 shows that $u_*(L)$ decreases with decreasing $|L|$ until it reaches its minimum value ($u_{*min}$) at $L = |L_{min}|$. According to (15), for $|L| < |L_{min}|$, $u_*(L)$ would increase monotonically with decreasing $|L|$, in such a way that $u_*(L) \to \infty$ for $|L| \to 0$. This behaviour occurs because, as $|L| \to 0$, the term between brackets on the right-hand side of (15) tends to infinity. This is a consequence of the physically unrealistic behaviour of MOST as $|L| \to 0$, producing singularities. For this reason, in Fig. 2 we have assumed that $u_*(L) = u_{*min}$, for $|L| \leq |L_{min}|$.

As can be seen in Fig. 2, $u_*(L)$ shows the expected physical behaviour (cf. Fig. 3.7 of Garratt 1992), approaching asymptotically (by design) $u_{*n}$ as $|L| \to \infty$, and decreasing monotonically with decreasing $|L|$. However, the approach to $u_{*n}$ as $|L| \to \infty$ is very gradual and $u_*$ only takes a value mid-way between the neutral and free-convection limits for a value of $|L|$ of several hundred metres. Furthermore, the minimum value reached by $u_*(L)$ is $u_{*min} = 0.17$ m s$^{-1}$ for $L_{min} = 3.4$ m; thus, $u_{*min} = u_{*fc}$ and $|L_{min}|$ almost coincides with $|L_{fc}| = 3.6$ m, determined previously (see Table 1). This result further confirms that the assumption of constant $(\partial U/\partial z)_{z_s}$ is realistic, and allows reliable estimates of $u_*$ to be obtained over the whole stability interval.

Although $u_{*fc}$, is thus a minimum value of $u_*$, it is generally not as low compared with $u_{*n}$ as might be expected. The case under consideration here, where $u_{*fc}/u_{*n} \approx 0.5$, which is not

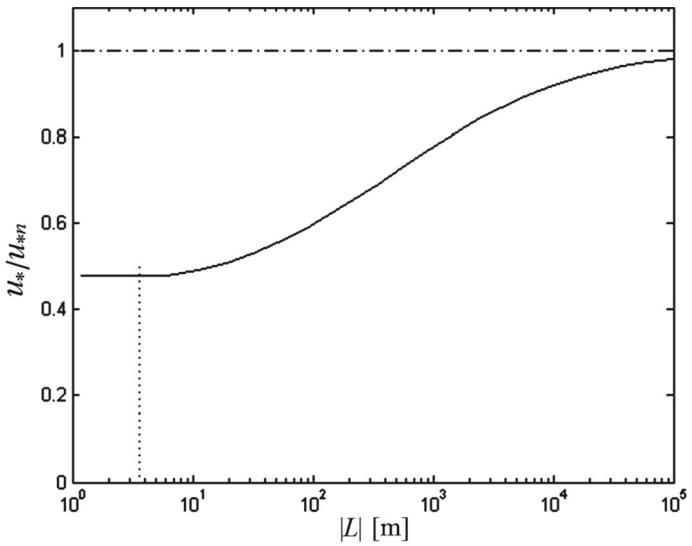


**Fig. 2** Friction velocity ($u_*$) as a function of $|L|$, obtained from (15) (*solid line*) and constant $u_*$ independent of the stability and equal to its value in the neutral regime ($u_{*n} = 0.35$ m s$^{-1}$) (*dash-dotted line*). Both quantities are normalized by $u_{*n}$. The *vertical dotted line* indicates the value of $L$ in the free-convection regime, $|L_{fc}| = 3.6$ m (see Table 1)

particularly low (see Sect. 3.1, Table 1), is a good example. This result ultimately suggests that a purely thermal regime is unlikely (it was not realized in the C94 measurements, in particular). For these reasons, under nearly free-convective conditions both $u_{*fc}$ and $L_{fc}$ differ substantially from zero, as is confirmed by the observations of K76 (see Table 2), and further corroborated for a very unstable surface-layer case by Steeneveld et al. (2005). This is what allows MOST to be used here for describing a highly convective ABL.

### 3.4 Flow Speed-Up Calculation

Since calculating $\Delta S\,(L)$ using the HLR model requires knowledge of $u_*\,(L)$, the main purpose of this section is to use the behaviour of $\Delta S(L)$ predicted by that model to indirectly assess the dependence on stability of $u_*(L)$ [and also of $z_s(L)$] established in the method proposed here, by comparison with values of $\Delta S$ measured over a wide range of $L$ by C94, and simulated numerically using the FLEX model.

Suppose that at a hilly location $\Delta S\,(L)$ needs to be estimated, assuming that the only available parameters are $z_0$ and the mean wind speed, $U(z)$, measured at a suitably low height such that, according to MOST, (11) is approximately valid for any $L$. Equation 11 can then be used for estimating $u_{*n}$. Once $z_0$ and $u_{*n}$ are known, the present method allows $z_s(L)$, then $u_*(L)$ and finally $\Delta S\,(L)$, for the whole unstable stratification parameter range, to be systematically obtained.

In the specific case under consideration here, first using as input parameters $u_{*n} = 0.35$ m s$^{-1}$ and $z_0 = 0.05$ m (from C94), $u_*\,(L)$ is calculated using the proposed method. Next, this $u_*\,(L)$ is used in the HLR model applied to flow over Cooper's ridge to calculate $\Delta S(L)$; $\Delta S(L)$ is also calculated assuming that $u_* = constant = u_{*n}$, regardless of the observed $L$. This simpler choice, often used for estimating $\Delta S(L)$ in flow over orography (e.g. W97), is what the present approach aims to improve. Finally, the $\Delta S$ values are com-

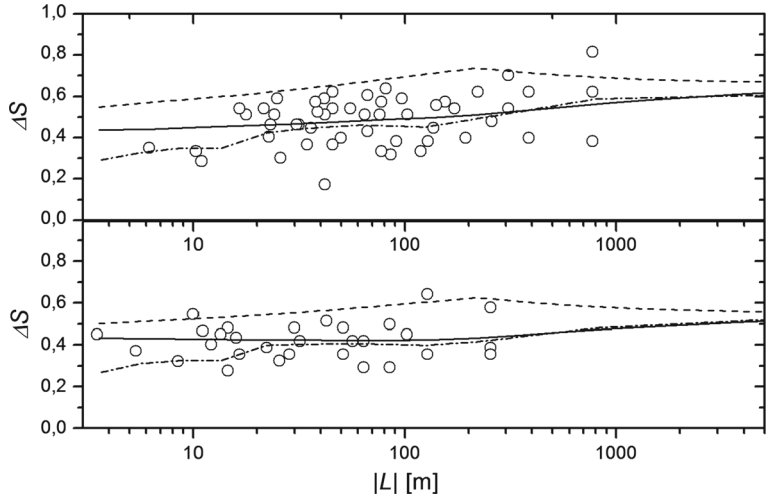


**Fig. 3** Variation of the fractional speed-up ($\Delta S$) as a function of stability, above the hill crest, at the heights $z = 8$ m (*top*) and $z = 16$ m (*bottom*). *Solid line*: $u_*$ computed using (15); *dotted line*: $u_*$ kept constant, regardless of the stability, and equal to the neutral ABL value ($u_{*n} = 0.35$ m s$^{-1}$); *dash-dotted line*: FLEX model; *symbols*: observations from C94

pared, for a range of $L$, using the HLR model results, the C94 measurements, and the FLEX model results.

For the sake of simplicity the HLR and FLEX models are not described in detail here; a brief description of the HLR model can be found in W97 or A09. The FLEX model is a microscale–mesoscale, non-linear and non-hydrostatic model, developed and validated against experimental and field data by Argaín (2003) and A09. This model has been tested and used extensively, namely by Teixeira et al. (2012, 2013a, b) for assessing analytical mountain-wave-drag predictions in 2D flows by comparison with numerical simulations.

All the numerical simulations presented here used a main grid of 160 × 364 points for a domain of 8000 m × 2000 m size. The horizontal domain extent is $20a$ ($7a$ upstream of the ridge maximum and $13a$ downstream), and from $z = 40$ m downward the level of grid refinement is gradually increased, and the lowest level is at a similar distance to the surface as the observations ( $\approx 0.15$ m). At the surface a no-slip condition is used, and $\left(\overline{w'\theta'}\right)_0$ and other turbulent quantities (turbulent kinetic energy, $E$, and rate of TKE dissipation $\varepsilon$), are specified for each $L$, by assuming that viscous dissipation balances shear and buoyancy production. At the upper boundary, constant $U$ and $\theta$ are prescribed, and the derivatives of $E$ and $\varepsilon$ are set to zero.

Observations, and both theoretical and numerical predictions of $\Delta S$ as a function of $|L|$, are shown in Fig. 3, for $z = 8$ m and $z = 16$ m. The HLR model is applied in two cases: a) $u_* = u_{*n}$, regardless of $|L|$ (dashed line), and b) the friction velocity is calculated for each $|L|$, using the method proposed here (15) (solid line).

The significant differences between the $\Delta S$ curves, obtained using the two different definitions of $u_*$, reveals that $\Delta S$ is very sensitive to the dependence of $u_*$ on $|L|$, as shown by A09 for the stable case. The results assuming $u_* = u_{*n}$ (dashed lines) overestimate the observations considerably. In both panels of Fig. 3, the improvement in the performance of the theoretical model, owing to the new method of calculating $u_*$ (solid lines), is significant over the whole stability interval. In general, this new method produces results much closer to

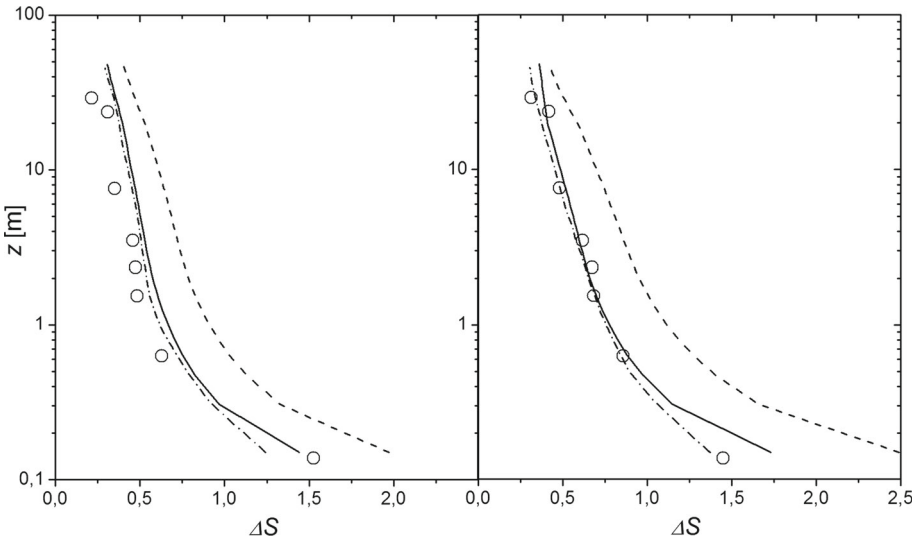


**Fig. 4** Profiles of the fractional speed-up ratio ($\Delta S$) above the hill crest, for $|L| = 33$ m (*left*) and $|L| = 222$ m (*right*). *Solid line*: $u_*$ computed using (15); *dashed line*: $u_*$ kept constant at $u_{*n} = 0.35$ m s$^{-1}$; *dash-dotted line*: FLEX model; *symbols*: observations from C94

both the field measurements (despite the considerable scatter in the data) and the numerical simulation results. $\Delta S$ calculated from the theoretical model with $u_*$ depending on $L$ has a rather flat variation with $|L|$, especially at $z = 16$ m, and although decreasing more substantially with $|L|$ at $z = 8$ m, slightly overestimates both the measurements and the numerical simulations for the lowest values of $|L|$.

Profiles of observations (C94), and both theoretical and numerical predictions of $\Delta S$ directly above the hill crest, for $|L| = 33$ m (left panel) and $|L| = 222$ m (right panel), are shown in Fig. 4; $|L| = 33$ m and $|L| = 222$ m correspond to strong and moderately weak unstable stratification, respectively. In both cases, the proposed method gives improved results both in comparison with the numerical model and with the field data, although it slightly overestimates the observations in the more unstable case. Nevertheless, a general decrease of $\Delta S$ as one shifts from the higher to the lower $|L|$ value is qualitatively reproduced. Given the precision of the measurements and flow assumptions, not too much importance should be attached to this overestimate, which also occurs in the numerical simulations (consistently, a similar discrepancy can be detected for the theoretical model on the far left of Fig. 3 at $z = 8$ m).

$\Delta S$ is much more severely overestimated, in both cases, by the profiles with a prescribed constant $u_* = u_{*n}$, due essentially to the significant fractional deviation between $u_{*n}$ and the more accurate value of $u_*$ determined from (15). This fractional deviation amounts to ≈45% for $|L| = 33$ m and to ≈ 35% for $|L| = 222$ m (see Fig. 2), but this does not translate into proportional deviations for $\Delta S$, as the value of $\Delta S$, where $u_*$ is calculated from (15), actually becomes closer to that where $u_* = u_{*n}$ as $|L|$ decreases (see Fig. 3). The fact that there is such a large difference in the results using $u_*(L)$ and $u_* = u_{*n}$ for the weakly unstable case might seem suspect, but Fig. 2 explains it, since for $|L| = 222$ m, $u_*(L)$ still differs very substantially from $u_{*n}$.

It should be pointed out that, at the lowest measurement level, $\Delta S$ should depend very weakly on $L$, because near enough to the ground the flow is always approximately neutral.

The overestimate of the measured $\Delta S$ at that level by the theoretical model for $|L| = 222$ m can probably be attributed to an inherent bias of the HLR model solution, noted by W97 and A09.

## 4 Summary and Conclusions

We have proposed a new method for estimating two scaling parameters of the ABL: the surface-layer height $z_s$ and the friction velocity $u_*$, as a function of stability (quantified by the Obukhov length scale $L$), for an unstable ABL. These two parameters are important for characterizing the unstable ABL, in particular its coupling with the overlying convective mixed layer. Moreover, a correct estimation of $u_*$, whose dependence on $L$ is often not accounted for in a physically consistent way, is crucial for producing accurate predictions of the speed-up ($\Delta S$) in flow over hills, which is relevant for a number of engineering applications.

Using a physical approach that is developed specifically for unstable conditions, via a combination of MOST and convective mixed-layer scaling, our model takes into account the fact that $z_s$ decreases as the unstable stratification becomes stronger, due to erosion of the surface-layer eddies by more energetic buoyancy-dominated eddies from the convective mixed layer. The model also takes into account the fact that $u_*$ decreases as the ABL becomes more unstable, attaining a minimum value, but does not, in general, approach zero in the free-convection limit, unless the wind vanishes completely (in which case the concept of $\Delta S$ loses its meaning). The variation of $u_*$ affects the turbulent fluxes of various properties, and consequently the mean profiles of those properties, including the wind speed $U(z)$, which determines the behaviour of $\Delta S$.

Procedures to obtain boundary-layer parameters in the neutral and free-convection regimes, and for bridging across these regimes to cover the complete unstable ABL parameter range, were developed and tested using available field data. The performance of the model was then evaluated more comprehensively, by comparing predictions of $\Delta S$ in unstable conditions, using the linear model of HLR incorporating the new friction velocity formulation, against measurements from C94, and numerical simulations of the FLEX mesoscale–microscale model. Agreement was found to be substantially improved relative to results where $u_*$ is held constant. This emphasizes the importance of accounting for the full dynamics of the unstable ABL, including the variation of $u_*$ and $z_s$ with stability, for correctly estimating $\Delta S$. The proposed method, whose possible applications are not limited to improving the calculation of $\Delta S$, should be seen as a preliminary step in the development of better tools for the parametrization of the unstable ABL. Further validation of this method by comparison with observations remains necessary.

**Acknowledgements** The authors thank two anonymous referees for insightful comments, which substantially improved this article. M.A.C.T. acknowledges the financial support of the European Commission, under Marie Curie Career Integration Grant GLIMFLO, contract PCIG13-GA-2013-618016. P.M.A.M. acknowledges the financial support of FCT, under Grant RECI/GEO-MET/0380/2012.

## Appendix 1: Accuracy of the $(\partial\theta/\partial z)_{z_s} = constant$ Approximation

In the present model, the form of $z_s(L)$ is established using the temperature gradient $\partial\theta/\partial z$, which can be obtained from (2) and (4), yielding

$$\frac{\partial\theta}{\partial z} = \theta_*'\left[1+\gamma_h\left(\frac{z}{|L|}\right)^{\alpha_1}\right]^{-\alpha_2} z^{-1}, \tag{18}$$

where $\theta_*' = Pr_t\theta_*/\kappa$ . According to (18), $\partial\theta/\partial z \to 0$ as $z \to \infty$. This is consistent with the assumption that $\theta = constant$ in the mixed layer, so at $z = z_s$ the derivative $(\partial\theta/\partial z)_{z_s}$ should be suitably small, and this smallness is exploited to obtain $z_s$. Note that a similar condition could be based on the mean velocity gradient (1), but we think that $\theta = constant$ is more reliable in the mixed layer, since $U(z)$ profiles may exhibit non-negligible shear above the surface layer, due to variation of the pressure perturbation induced by the orography with height or the Coriolis force. Taking this into account, the ratio

$$\Psi(z_s, L) = \frac{(\partial\theta/\partial z)_{z_s}}{(\partial\theta/\partial z)_{z_{0\theta}}} = \left[\frac{1+\gamma_h(z_s/|L|)^{\alpha_1}}{1+\gamma_h(z_{0\theta}/|L|)^{\alpha_1}}\right]^{-\alpha_2}\frac{z_{0\theta}}{z_s}, \tag{19}$$

implicitly determines $z_s(L)$, if the form of the function $\Psi(z_s, L)$ is known. In (19) $(\partial\theta/\partial z)_{z_s}$ and $(\partial\theta/\partial z)_{z_{0\theta}}$ are obtained by evaluating (18) at $z_s$ and the thermal roughness length, $z_{0\theta}$, respectively. As defined by (19), $\Psi(z_s, L)$ varies monotonically from 1 to zero as $z_{0\theta}/z_s$ decreases. Moreover, $\Psi(z_s, L)$ depends only weakly on $L$: by substituting $L_{fc}, z_{sfc}, z_{sn}$ and $L_n = \infty$ (see Sect. 3.1, Table 1) into (19) we may calculate the ratio $\Gamma = \Psi(z_{sn}, L \to -\infty)/\Psi(z_{sfc}, L_{fc}) \approx 0.6$, which is $\approx 1$.

The limits of $\Psi(z_s, L)$ at the theoretical extremes of the stability interval are, respectively,

$$\Psi_{sfc} = \Psi(z_{sfc}, L \to 0) = \lim_{|L|\to 0}\Psi(L) = \left(\frac{z_{0\theta}}{z_{sfc}}\right)^{\alpha_1\alpha_2+1}, \tag{20}$$

$$\Psi_{sn} = \Psi(z_{sn}, L \to \infty) = \lim_{|L|\to\infty}\Psi(L) = \frac{z_{0\theta}}{z_{sn}}. \tag{21}$$

For both strongly and weakly unstable flows, (20)–(21) suggest that $\psi(z_s, L) \propto (z_{0\theta}/z_s)^{\alpha}$, where $\alpha$ is a dimensionless constant. Taking this result into account, we hypothesize that this form holds for the whole stability interval, yielding the following approximate definition for $\psi(z_s, L)$,

$$\Psi(z_s, L) = \alpha_{\Psi 2}\left(\frac{z_{0\theta}}{z_s}\right)^{\alpha_{\Psi 1}}, \tag{22}$$

where $\alpha_{\Psi_1}$ and $\alpha_{\Psi_2}$ are dimensionless constants. These two constants can be determined by taking the limits of (22) in the free-convection and neutral regimes, and comparing the corresponding expressions with (20) and (21), respectively. This produces a set of two equations, which may be solved for $\alpha_{\Psi_1}$ and $\alpha_{\Psi_2}$, yielding

$$\alpha_{\Psi 1} = \ln\left[\frac{\Psi(z_{sn}, L\to\infty)}{\Psi(z_{sfc}, L_{fc})}\right]\Big/\ln\left(\frac{z_{sfc}}{z_{sn}}\right) \qquad \alpha_{\Psi 2} = \Psi(z_{sfc}, L_{fc})\left(\frac{z_{0\theta}}{z_{sfc}}\right)^{-\alpha_{\Psi 1}} \tag{23}$$

By combining (19) and (22), (14) is obtained.

## Appendix 2: Accuracy of the $(\partial U/\partial z)_{z_s} = constant$ Approximation

Here we show that the approximation $(\partial U/\partial z)_{z_s} = constant$, used in Sect. 2.4 for evaluating $u_*$, is supported by measurements. Let us consider the following ratio, by using MOST,

**Table 2** CBL parameters measured by Kaimal et al. (1976)

| Run | $u_{*fc}$ (m s$^{-1}$) | $\lvert L_{fc}\rvert$ (m) | $z_{ifc}$ (m) | $w_*$ (m s$^{-1}$) | $w_*/z_{ifc}$ (s$^{-1}$) | $\beta_{MOST}$ |
|---|---|---|---|---|---|---|
| 6A1 | 0.24 | 5.7 | 2095 | 2.43 | $1.16 \times 10^{-3}$ | 1.1 |
| 6A2 | 0.23 | 6.4 | 2035 | 2.21 | $1.09 \times 10^{-3}$ | 1.3 |

Columns 6 and 7 show, respectively, $w_*/z_{ifc}$, and $\beta_{MOST}$, calculated from the data [the second quantity by using (24)]

$$\beta_{MOST} = \frac{(\partial U/\partial z)_{z_{sn}}}{(\partial U/\partial z)_{z_{sfc}}} = \underbrace{\left(\frac{c_{fc}\beta_1|f|}{c_{SL}c_{zin}}\right)}_{\alpha_5} \frac{|L_{fc}|}{u_{*fc}}, \tag{24}$$

where $\beta_1 = \left(1 + \gamma_m c_{fc}^{\alpha_1}\right)^{\alpha_2}$, and obtained by combining (1), (4), (6), (12) and (13). Using parameters from C94 (see Sect. 3.1) we obtain $\alpha_5 = 0.0466\ \mathrm{s}^{-1}$; for the values of $L_{fc}$ and $u_{*fc}$ shown in Table 1, this yields $\beta_{MOST} = 0.99$. The remarkable closeness of this value to 1 is fortuitous, although it obviously depends on the values adopted for $c_{zin}$, $c_{fc}$ and $c_{SL}$. For checking further the approximation $\beta_{MOST} \approx 1$ we use the K76 observations (keeping the same $\alpha_5$), which were carried out in a daytime well-mixed CBL, with evidence of significant heat and momentum entrainment through the capping inversion.

Table 2 shows CBL parameters obtained by K76, corresponding to the runs with the smallest values of $|L|$, typical of nearly free-convection regimes. As can be seen, the values of $\beta_{MOST}$ are close to 1, corroborating the hypothesis $\beta_{MOST} \approx 1$. Moreover, column 6 supports (10) proposed by Venkatram (1978), since $c_5 = w_*/z_{ifc}$ varies within a narrow range. Venkatram (1978) estimated $c_5 = 1.12 \times 10^{-3}\ \mathrm{s}^{-1}$, which is quite close to both values shown in Table 2. Therefore, the assumption that $c_5$ is a constant is plausible.

If the assumption $\beta_{MOST} = 1$ is accepted, (24) defines a relationship between $\alpha_5$, $|L_{fc}|$ and $u_{*fc}$, and if parameters $c_{fc}$ and $c_{zin}$ are assumed to be non-adjustable, this is equivalent to a relation between $|L_{fc}|$, $u_{*fc}$ and $c_{SL}$. Equation 13 is only applicable if $|L| \to \infty$ (a rarely observed situation), so the parameter $c_{zin}$ may have a considerable uncertainty. Garratt (1992) and Zilitinkevich et al. (2012) discuss this topic at length. It would be interesting to explore the constraint defined by (24) further to develop relations other than (13) for estimating $z_{in}$, but that is beyond the scope of the present study.

We also carried out a similar analysis using the classical free-convection formulation of Prandtl (1932) for the mean velocity gradient,

$$\left(\frac{\partial U}{\partial z}\right)_{z_{sfc}} = \frac{c_u u_{*fc}(\kappa|L_{fc}|)^{1/3}}{z_{sfc}^{4/3}} = \frac{c_u \kappa^{1/3}}{c_{fc}^{4/3}} \frac{u_{*fc}}{|L_{fc}|}, \tag{25}$$

where $c_u = 1.7$. In this case we obtain a ratio $(\partial U/\partial z)_{z_{sfc}}/(\partial U/\partial z)_{z_{sn}}$ with a similar parameter dependence as (24) and $\alpha_5 = 0.0453\mathrm{s}^{-1}$. The proximity between the values of $\alpha_5$ obtained using both formulations for $(\partial U/\partial z)_{z_{sfc}}$ confirms that the MOST formulation adopted here is physically consistent, hence it may be used to describe the free-convection regime.

## References

Argaín JL (2003) Modelação de Escoamentos Atmosféricos: Efeitos Orográficos e de Camada Limite (in Portuguese). Ph.D. Thesis, Universidade do Algarve, 275 pp

Argaín JL, Miranda PMA, Teixeira MAC (2009) Estimation of the friction velocity in stably stratified boundary-layer flows over hills. Boundary-Layer Meteorol 130:15–28
Businger JA (1973) A note on free convection. Boundary-Layer Meteorol 4:323–326
Coppin PA, Bradley EF, Finnigan JJ (1994) Measurements of flow over an elongated ridge and its thermal stability dependence: the mean field. Boundary-Layer Meteorol 69:173–199
Deardorff JW (1970) Convective velocity and temperature-scales for the unstable planetary boundary layer. J Atmos Sci 27:1211–1213
Garratt JR (1992) The atmospheric boundary layer. Cambridge University Press, Cambridge, 316 pp
Hunt JCR, Leibovich SL, Richards KJ (1988) Turbulent shear flows over low hills. Q J R Meteorol Soc 29:16–26
Kader BA, Yaglom AM (1990) Mean fields and fluctuation moments in unstably stratified turbulent boundary layers. J Fluid Mech 212:637–662
Kaimal JC, Wyngaard JC, Haugen DA, Cote OR, Izumi Y, Caughey SJ, Readings CJ (1976) Turbulence structure in the convective boundary layer. J Atmos Sci 33:2152–2169
McNaughton KG (2004) Turbulence structure of the unstable atmospheric surface layer and transition to the outer layer. Boundary-Layer Meteorol 112:199–221
Prandtl L (1932) Meteorologische anvendungen der strömungslehre. Beitr Phys Fr Atmos 19:188–202
Rossby CG, Montgomery RB (1935) The layers of frictional influence in wind and ocean currents. Pap Phys Oceanogr Meteorol 3:101
Schumann U (1988) Minimum friction velocity and heat transfer in the rough surface layer of a convective boundary layer. Boundary-Layer Meteorol 44:311–326
Steeneveld GJ, Holtslag AAM, DeBruin HAR (2005) Fluxes and gradients in the convective surface layer and the possible role of boundary-layer depth and entrainment flux. Boundary-Layer Meteorol 116:237–252
Stull RB (1988) An introduction to boundary-layer meteorology. Kluwer Academic Publishers, Dordrecht, 670 pp
Stull RB (2011) Meteorology for scientists and engineers, 3rd edn. University of British Columbia, Vancouver
Sykes RI, Henn DS, Lewellen WS (1993) Surface-layer description under free-convection conditions. Q J R Meteorol Soc 119:409–421
Teixeira MAC, Argaín JL, Miranda PMA (2012) The importance of friction in mountain wave drag amplification by Scorer parameter resonance. Q J R Meteorol Soc 138:1325–1337
Teixeira MAC, Argaín JL, Miranda PMA (2013a) Drag produced by trapped lee waves and propagating mountain waves in a two-layer atmosphere. Q J R Meteorol Soc 139:964–981
Teixeira MAC, Argaín JL, Miranda PMA (2013b) Orographic drag associated with lee waves trapped at an inversion. J Atmos Sci 70:2930–2947
Venkatram A (1978) Estimating the convective velocity scale for diffusion applications. Boundary-Layer Meteorol 15:447–452
Von Engeln A, Teixeira J (2013) A planetary boundary-layer height climatology derived from ECMWF reanalysis data. J Clim 26:6575–6590
Weng W (1997) Stably stratified boundary-layer flow over low hills: a comparison of model results and field data. Boundary-Layer Meteorol 85:223–241
Weng W, Taylor PA (2003) On modelling the one-dimensional atmospheric boundary layer. Boundary-Layer Meteorol 107:371–400
Wilson DK (2001) An alternative function for the wind and temperature gradients in unstable surface layers. Boundary-Layer Meteorol 99:151–158
Zilitinkevich SS (1995) Non-local turbulent transport: pollution dispersion aspects of coherent structure of convective flows. In: Power H, Moussiopoulos N, Brebbia CA (eds) Air pollution III Vol 1. Air pollution theory and simulation, computational mechanics publications. Southampton, pp 53–60
Zilitinkevich SS, Hunt JCR, Grachev AA, Esau IN, Lalas DP, Akylas E, Tombrou M, Fairall CW, Fernando HJS, Baklanov AA, Joffre SM (2006) The influence of large convective eddies on the surface-layer turbulence. Q J R Meteorol Soc 132:1423–1456
Zilitinkevich SS, Tyuryakov SA, Troitskaya YI, Mareev EA (2012) Theoretical models of the height of the atmospheric boundary layer and turbulent entrainment at its upper boundary. Izv Atmos Ocean Phys 48:133–142